Thermochimica Acta 670 (2018) 18–26

Contents lists available at ScienceDirect

Thermochimica Acta

journal homepage: www.elsevier.com/locate/tca

Thermal and kinetics of the degradation of chitosan with different deacetylation degrees under oxidizing atmosphere

M. Mar Villar-Chavero*, Juan C. Domínguez, M. Virginia Alonso, Mercedes Oliet, Francisco Rodriguez

Chemical Engineering and Materials Department, Complutense University of Madrid, Av. Complutense S/N, 28040, Madrid, Spain

ARTICLE INFO

Keywords:
Chitosan
Deacetylation degree
Thermal stability
Isoconversional method
DAEM model

ABSTRACT

The degradation process of chitosan with degrees of deacetylation (DD) varying from 54 to 84% was investigated by thermogravimetric analysis at different heating rates under air atmosphere. The chitosan with DD of 54% presented the highest thermal stability and slower changes in its structure as the temperature was increased, according to the infrared spectroscopy analyses.

The activation energies (E_a) of the degradation process were estimated by the Flynn-Wall-Ozawa and the Vyazovkin isoconversional methods, obtaining values between 90 and 319 kJ/mol. The 3R-Gaussian distributed activation energy (3R-Gaussian DAEM) model was applied and adjusted successfully to the experimental data. In addition, DAEM model allowed to determine the E_a associated to each degradation reaction stage of chitosan (between 163–346.3 kJ/mol), in contrast to isoconversional methods. Consequently, the 3R-Gaussian DAEM model is a suitable option to describe the kinetics of chitosan degradation process.

1. Introduction

Chitosan is a polysaccharide used in many fields, such as cosmetic industry, water engineering, food industry, pharmacy, and medicine due to its physico-chemical and biological good properties: antioxidant, adsorption enhancer, anticholesterolemic, antimicrobial, analgesic, hemostatic, etc. [1–3]. This polysaccharide is a lineal copolymer of β–(1-4) linked 2–acetamido–2–deoxy–β–D–glucopyranose or *N*–acetyl–D–glucosamine (GlcNAc) and 2–amino–2–deoxy–β–D–glucopyranose or D–glucosamine (Glc); and it is obtained by deacetylation of chitin [4]. Chitin is easily accessible since it comes, principally, from wastes of seafood processing industries [5].

One of the most important parameters for establishing the physico-chemical identity of chitosan is the degree of deacetylation (DD), which is defined as the molar fraction of the units D–glucosamine presents in the polymeric chain. When the DD is above 50%, the polymer is called chitosan, and when the DD is below of this percentage, it is known as chitin [6]. Therefore, chitosan with different DD has varying physico-chemical properties [4,7,8].

The study of the thermal degradation of chitosan is very useful to establish its thermal stability, to understand the structural changes and to determine the reactions that take place during this process. This knowledge is of great importance in order to define the applications of chitosan [9]. In this line, the thermal degradation of chitosan is relevant for the design and planning of the industrial processes to which chitosan is exposed to obtain, for instance, membranes, drugs, flocculants, reinforcement chemical or physical, etc. [9–14].

Several authors have studied the pyrolysis of chitosan with different degrees of deacetylation by using thermogravimetric analysis [11,15–17]. These studies concluded that the pyrolysis of chitosan occurs in two steps. The first one is due to the deacetylation and depolymerization processes, while the second one is related to the residual decomposition reactions produced in inert conditions. Furthermore, in terms of kinetics of the degradation process, these authors reported that the activation energies (E_a) estimated for chitosans with lower DD are greater than for chitosans with higher DD, i.e. in the latter case chitosans are less thermally stable [18–20]. However, there is little studies about the kinetics and thermal properties of the thermal degradation of chitosan as a function of DD in oxidizing atmosphere.

The present work aims to investigate the effect of the DD of chitosan on its thermal stability under air atmosphere, as well as comparing the obtained kinetic parameters of the degradation processes of chitosan by isoconversional methods and a multi-reaction distributed activation energy (DAEM) model. For this purpose, chitosans with different DD

* Corresponding author at: Chemical Engineering and Materials Department, Faculty of Chemistry, Complutense University of Madrid, Av. Complutense S/N, 28040, Madrid, Spain.
E-mail address: mdm.villar@ucm.es (M.M. Villar-Chavero).

https://doi.org/10.1016/j.tca.2018.10.004
Received 10 July 2018; Received in revised form 28 September 2018; Accepted 5 October 2018
Available online 09 October 2018
0040-6031/

(between 54-84%) were obtained from chitin thorough a deacetylation process. Fourier Transform infrared spectroscopy (FTIR) was used to establish the DD of the produced chitosans and study the changes in their chemical structure during the thermal degradation process. The experimental data of the degradation process were obtained by thermogravimetric analysis (TGA). To determine the crystallinity of the samples X-Ray Diffraction (XRD) was utilized. The Flynn-Wall-Ozawa (FWO) and Vyazovkin (VYA) isoconversional methods were used to estimate the activation energies as a function of the conversion of the thermal degradation of chitosans. A multi-reaction DAEM model of three reaction stages was proposed in order to model the behavior during the degradation process, as well as to determine the kinetic parameters of each reaction stage.

2. Kinetic study: Theory

Generally, chemical reactions of the degradation processes are described by a single step kinetic equation [21], Eqs. (1) and (2):

$$d\alpha/dt = k(T)\cdot f(\alpha) \tag{1}$$

$$\alpha(t) = \frac{w_0 - w_t}{w_0 - w_f} \tag{2}$$

where t is time; $\alpha(t)$ is the conversion, defined as the ratio between the instant mass loss and the total mass loss; w_0 and w_f and are the initial and final masses of the sample, respectively; w_t is the mass at time t; $f(\alpha)$ is the process mechanism function; and $k(T)$ is the rate constant, usually assumed to follow an Arrhenius equation, Eq. (3):

$$k(T) = k_0\cdot\exp\left(-\frac{E_a}{R\cdot T}\right) \tag{3}$$

where k_0 is the pre-exponential factor, E_a is the activation energy, T is the absolute temperature, and R is the universal gas constant.

2.1. Isoconversional methods

One of the major problems in kinetic study is the knowledge of the kinetic model due to several decomposition reactions that take place during a degradation process. For this reason, isoconversional methods, also called model–free kinetics methods, are widely used because they do not assume a kinetic model [21]. In this work, two isoconversional methods were employed: the Flynn-Wall-Ozawa [22,23] and Vyazovkin methods [24–26]. Henceforth, these methods will be referred FWO and VYA, respectively. The FWO method is described by Eq. (4):

$$\ln(\beta) = A - 1.052\frac{E_a}{R\cdot T_\alpha} \tag{4}$$

where β is the heating rate, A is a constant and T_α is the temperature at a certain conversion. This method is one of the most frequently used in the literature to determine activation energies of degradation processes of chitosan and their derivates [11,13,16,27].

The VYA method is more accurate due to directly performing numerical integration [21] by minimizing the Eq. (5):

$$\Phi(E_a) = \sum_{i=1}^{n}\sum_{j\neq i}^{n}\frac{I(E_a, T_{\alpha,i})\beta_j}{I(E_a, T_{\alpha,j})\beta_i} \tag{5}$$

in which $I(E_a,T_\alpha)$, the temperature integral, is defined by Eq. (6):

$$I(E_a, T_\alpha) = \int_{T_{\alpha-\Delta\alpha}}^{T_\alpha}\exp\left(-E_a/R\cdot T\right)dT \tag{6}$$

The temperature integral is calculated to obtain the activation energy at each given value of conversion.

2.2. DAEM model

Another way to address the kinetic study of degradation processes is the DAEM model. This model is an alternative to isoconversionals methods and it is found in the literature to describe the kinetics of degradation of different biopolymers, including chitosan and chitin [14]. The DAEM model assumes that the degradation process occurs in several independent and parallel n^{th} order reactions [28,29]. It is described by Eq. (7), when the reaction order is 1 and the process is non-isothermal:

$$\alpha(T) = \int_0^\infty\left\{1 - \exp\left[-\frac{k_0}{\beta}\int_0^T\exp\left(-\frac{E_a}{R\cdot T}\right)dT\right]\right\}f(E_a)dE_a \tag{7}$$

Due to that each reaction has a different activation energy, the degradation process presents a distribution of activation energies, $f(E_a)$, usually described by a continuous distribution function. The Gaussian distribution is one of the most commonly used [30], which is indicated in Eq. (8):

$$f(E_a) = \frac{1}{\sigma\sqrt{2\pi}}\exp\left[-\frac{(E_a - E_{a0})^2}{2\sigma^2}\right] \tag{8}$$

where E_{a0} is the mean activation energy, and σ is the standard deviation of the Gaussian distribution.

A natural sample may contain several components or can be described by pseudocomponents [31,32]. In this case, a multi-reaction DAEM model can be applied to total conversion generally as a linear combination of the degradation of the individual components (or pseudocomponents), described by Eq. (9):

$$\alpha(T) = \sum_{j=1}^{n} c_j\alpha_j(T)\Big/\sum_{j=1}^{n} c_j \tag{9}$$

where c_j is the fraction of each component of the sample that is reacting, $\alpha_j(T)$ is the conversion for each component of the sample, and n is the number of individual components of the sample.

3. Materials and methods

3.1. Materials and reagents

Chitin powder from Alaska snow crab shells was purchased from G.T.C. Bio Corporation (China) and it was used without any further purification. Sodium hydroxide pellets and potassium bromide were acquired from Panreac Applichem.

3.2. Deacetylation of the chitin and determination of the degree of deacetylation

Chitin was mixed with different NaOH solutions (10 g per 300 mL of alkali solution). Concentrations of 37.1, 37.9, 39.3, 45 and 52% of NaOH were used to obtain chitosan with different DD. The deacetylation processes were carried out in a 500 mL flat bottom flask for 3 h at 105 °C, under stirring at 900 rpm. After filtration, obtained chitosans were washed until neutral pH and dried in an oven for 3 h at 100 °C. The samples were milled in a MM301 Retsch ball mill and sieved (particle size < 180 μm) in order to obtain homogenized ones.

The DD of chitin was 5.2%, determined according to Ottey, Vårum and Smidsrød [33] and Raymond, Morin and Marchessault [34] using ^{13}C CP/MAS NMR spectroscopy (Fig. S.1). Conversely, the DD of obtained chitosans were determined by Fourier Transform infrared spectroscopy (FTIR). FTIR spectra were recorded with a FT/IR-4600 Jasco spectrophotometer using the KBr method. The pellet was prepared from a mixture of sample and KBr (1:100 ratio). The spectra were acquired by accumulation of 64 scans and a wavenumber range of 4000-400 cm^{-1}, with a resolution of 2 cm^{-1}. The DD was calculated applying Eq. (10),

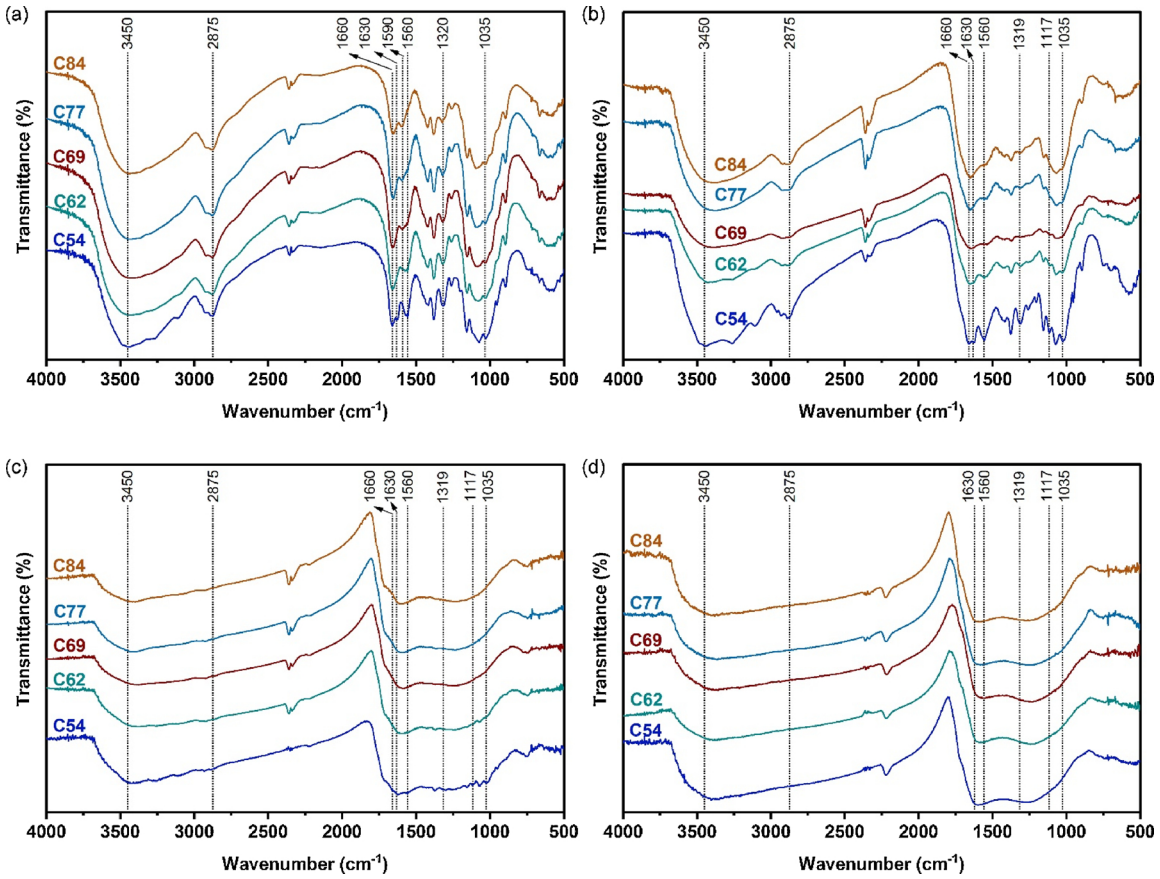

Fig. 1. FTIR spectra of C54, C62, C69, C77, and C84 at room temperature (a), 290 (b), 340 (c), and 500 °C (d).

proposed by Brugnerotto, Lizardi, Goycoolea, Argüelles-Monal, Desbrieres and Rinaudo [35], in which A_{1320}/A_{1420} represents the ratio of absorbance of the bands 1320 and 1420 cm^{-1}, respectively.

$$A_{1320}/A_{1420} = 0.3822 + 0.03133 \cdot DD \quad (10)$$

3.3. Structural changes during the process of chitosan degradation

FTIR spectroscopy was also employed to determine the changes in the chemical structure of the chitosans during their thermal degradations. First, the chitosan samples were degraded in a Mettler-Toledo TGA/STDA 851^e under air atmosphere (flow rate of 20 mL/min) using temperature profiles that started from 30 °C and reached 290, 340, and 500 °C at a heating rate of 10 °C/min. After the degradation, the samples were stored in a desiccator for 15 min at room temperature. The KBr method was applied under the same conditions of preparation and measure than in the determination of DD of chitosans.

3.4. Determination of the crystallinity of chitosans

The crystallinity of the obtained chitosans, as well as the chitin raw material, was evaluate in order to determine the percentage of the crystalline part (CrI) of the biopolymers. For that purpose, a Philips X'Pert MDP X-Ray diffractometer was used with Cu-Kα radiation at 45 kV and 40 mA, and the relative intensity was recorded in the scattering range (2θ) between 2 and 40° with a speed 0.6°/min. CrI was calculated according to Eq. (11) proposed by Focher, Beltranme, Naggi and Torri [36]:

$$CrI = (I_{110} - I_{am}) \cdot 100 / I_{110} \quad (11)$$

where I_{110} is the maximum intensity of the 110 lattice diffraction (at $2\theta \approx 20°$), and I_{am} is the intensity of amorphous diffraction in the same units than I_{110} (at $2\theta \approx 16°$).

3.5. Evaluation of the thermal stability of the chitosans

The thermogravimetric measurements were carried out in the TGA instrument under air atmosphere (flow rate of 20 mL/min). The analyses were performed in alumina crucibles (70 μL) and the weight of the sample was between 8 and 11 mg. All samples were heated from 30 to 950 °C at heating rates of 6, 8, 10, 12 and 14 °C/min. Thermal stability was defined as the temperature at 25% of conversion on dry basis ($T_{25\%}$). Three samples were measured at each heating rate.

3.6. Determination of the kinetic parameters of the degradation process

The data of TGA analyses were treated with Matlab R2014b software to obtain the activation energies of the degradation process of chitosan by FWO and VYA isoconversional methods. In addition, a multi-reaction DAEM model of three reaction stages (henceforth 3R-Gaussian DAEM model) was also applied to the TGA data to obtain the kinetic parameters (activation energies and pre-exponential factors) of the degradation reaction steps. The parameters of the 3R-Gaussian DAEM model were estimated using a Levenberg-Marquardt algorithm [37], i.e. a non-linear least-squares minimization algorithm, evaluating the model for 100 equispaced conversion values.

4. Results and discussion

The DDs of the chitosans were calculated through the spectra acquired by FTIR (Fig. 1.a) using the Eq. (10). For the NaOH concentrations of 37.1, 37.9, 39.3, 45 and 52%, the DDs values were 54, 62, 69, 77, and 84%, respectively. In this work, chitosans are labeled according to their DD as C54, C62, C69, C77 and C84.

4.1. Structural characterization in the degradation process

FTIR spectra for the obtained chitosans at room temperature are shown in Fig. 1.a, in which different representative bands of chitosan are indicated. At room temperature, C54 sample exhibited a band at 3450 cm^{-1} that corresponds to O–H and N–H stretchings [9]. The region spectral between 3000 and 2800 cm^{-1}, is associated with symmetric and asymetric stretchings of C-H from the ring and from CH_2OH and CH_3 groups. This sample presented a doublet at 1660 and 1630 cm^{-1}, attributed to C–O stretch of acetyl group [39]. Due to C–N–C strech and the NH bending vibration, a characteristic GlcNAc units band at 1560 cm^{-1} is found in the C54 FTIR spectrum. Likewise, the band at 1320 cm^{-1} (symetric or asymmetric CH_2 stretching) is a typical signal of the GlcNAc units. The absoption band at 1035 cm^{-1} corresponds with the bridge O stretch [16,39]. By increasing the DD, some of these representavite bands were altered in comparation with the C54 spectrum. Specifically, the signals between 3000-2800 cm^{-1}, except the band at 2875 cm^{-1}, decreased slightly for C62-C84 samples as result of the CH_3 elimination from the acetyl group of GlcNAc unit [38]. Moreover, the signal at 1630 cm^{-1} was not found in these spectra. In addition, these samples exhibited a emerging band at 1590 cm^{-1} (NH_2 bending vibration in amino group) due to the conversion of secundary amines into primary amines in the deacetylation process. For the same reason, the intensity of the band at 1560 cm^{-1} decreased as the DD was increased from 62 to 78; for the sample C84, the one with the highest DD, this signal was not found. Finally, the band at 1320 cm^{-1} decreased when the DD increased due to the less presence of the acetyl goups [40].

The temperatures selected to study the structural characterization in the degradation process were 290, 340, and 500 °C. FTIR spectra recorded at these temperatures of degradation are presented in Fig. 1.b–d, respectively. At 290 °C for all studied samples, the bands at 3450 cm^{-1} decreased due to the dehydration of the samples; however, the diminution of the bands at 1660 and 1560 cm^{-1} was due to the deacetylation process that took place during the degradation of chitosan [9]. On the other hand, a new band at 1117 cm^{-1} (C–O–C stretch) appeared in the spectrum of the C54 and C62. This change was due to the result of depolymerization reactions and the cleavage glycosidic linkages attributable to the oxidation process [9,13]. At 340 °C, all the described bands practically disappeared for all samples, including the signal at 2875 cm^{-1} due to degradation to the pyranose ring [15], although for C54 sample the diminution was lower than for the other samples. The spectra recorded at 500 °C did not show important differences, indicating the samples reacted to form a residue composed of carbonaceous structures [41].

FTIR analysis at different temperatures suggested that chitosan with the lowest DD (C54) was more thermally stable than the others, since its chemical structure changed less sharply with increasing temperature (Fig. 1.a–d).

4.2. Thermal stability

The thermal stability and the degradation stages of chitosans were analyzed employing the thermograms obtained from the TGA tests and the derivatives from these curves (DTG). The curves of the chitin raw material, C54 and C84 samples tested at a heating rate of 10 °C/min are shown in Fig. 2; values obtained at temperatures higher than 700 °C are not shown because mass loss remained constant for all the samples.

Four peaks were found in the DTG curve of the chitin associated to four stages (Fig. 2.a). The first stage, between 30–130 °C, is attributed to water desorption [42]. The second and third peak overlapped in the range 130–400 °C, were due to the decomposition of polymer chains through deacetylation and cleavage of glycosidic linkages; at first, the degradation of chitosan D–glucosamine (Glc) units was produced (130–310 °C, with a reached conversion in dry basis of the 33%) and later decomposition of chitosan *N*–acetyl–D–glucosamine (GlcNAc) units took place at a temperature range of 310–400 °C, with a conversion between 33 and 64% [9,20,42]. The last stage of thermal degradation occurred between 400 and 600 °C, and it was attributed to total degradation of chitosan ring and decomposition of the residual carbon [9,43].

The DTG curve of C84 sample was similar to that obtained for chitin (Fig. 2.c), being the mechanism of the degradation the same for both samples [9,20]. The same fact was also observed in C62, C69, and C77 curves (Fig. S.2). An important difference between chitin and C84 sample was the temperature of the maximum velocity reached in the overlapped of the degradation of Glc and GlcNAc units (second and third peaks). For chitin, this velocity was achieved at 332.6 °C, related to the degradation of GlcNAc units; and for C84 sample was 300 °C, consistent with the degradation of Glc units of chitosan. Therefore, the influence of DD on the degradation process was significant.

Based on these results, the degradation behavior of the C54 sample was intermediate between chitin and C84 (Fig. 2.b). In this case, in the C54 thermogram were discerned two peaks in the 130–400 °C interval due to the similar amount of GlcNAc and Glc units in the polymer (54 and 46% of GlcNAc and Glc, respectively). The first of these peaks related to the degradation of Glc units, and the second with the degradation of GlcNAc units (maximum velocity of degradation at 300 and 343 °C, respectively), as stated above.

In all cases, increasing the heating ramp resulted in shifting the peaks of the stages to higher temperatures because of the heat transfer lag [9].

The thermal stabilities of the chitin employed as raw material and the chitosans with different DD were assessed by $T_{25\%}$ (on dry basis) because it corresponded with the second stage of the process of degradation (degradation of the Glc units), and therefore the DD was considered. All values for each used heating rate are shown in Table 1 together with the results of crystallinity obtained from XRD diffractograms (Fig. S.3).

Chitin raw material exhibited the highest thermal stability of the studied samples, between 309 and 325.1 °C, as shown in Table 1. It was followed by C54 sample, which presented thermal stabilities higher than the remaining chitosans (between 298.5–313.7 °C). This is in agreement with the results obtained from the study of the structural changes in the degradation process, since the C54 sample presented less structural changes than the other chitosans as temperature was increased (Section 4.1). By increasing the DD from 69 to 84%, the thermal stability of samples remained almost constant (e.g. 293.9–299.7 °C, for the 10 °C/min heating rate).

These results, together the obtained TGA thermograms (Fig. 2), suggest that the Glc and GlcNAc units forming the chitosan have different thermal stability. This fact is caused by the crystallinity of the GlcNAc units, a greater amount of these units in the polymer (less DD) causes a higher crystallinity index (being this index maximum for chitin raw material, 95.7%), and therefore the thermal stability of chitosan is increased [1,14,44]. However, for DD values higher than 62%, the crystallinity remained constant, between 72.3 and 75.7% for the C69, C78 and C84 samples. For this reason, there was not variation of the thermal stabilities of these samples. Interestingly, Nam, Park, Ihm and Hudson [20] observed that chitosans with different DD (59, 76 and 85%) presented similar thermal stabilities among them under N_2 atmosphere.

4.3. Kinetic study of thermal degradation of chitosans

4.3.1. Isoconversional methods

The activation energies as a function of the reached conversion obtained by applying of FWO and VYA methods are showed in Fig. 3. The obtained results demonstrated the strong dependence of the conversion on the activation energies for all the obtained chitosans and chitin.

At the beginning of the thermal degradation up to 70% conversion,

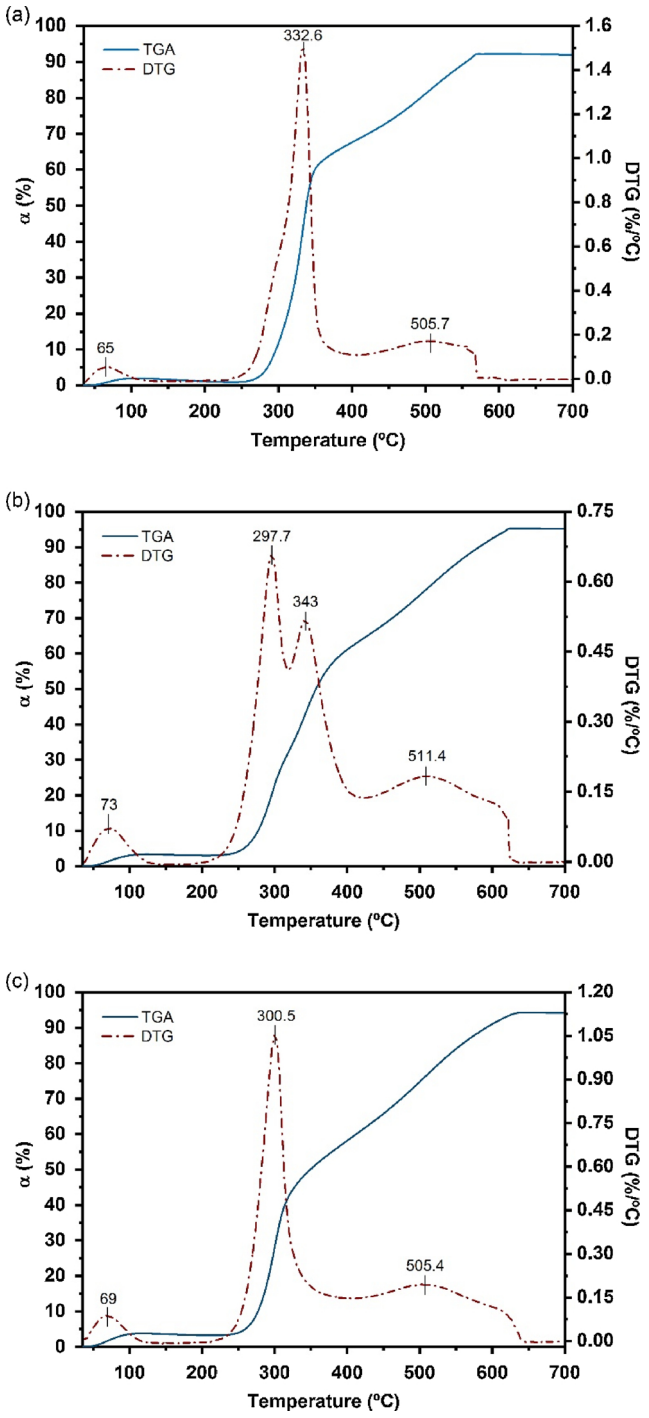

Fig. 2. TGA measurements and DTG curves of chitin (a), C54 (b), and C84 (c) at a heating rate of 10 °C/min.

the activation energies of chitin raw material, calculated by FWO method, remained constant (≈ 150 kJ/mol), and by VYA method ranged between 168.9–207.3 kJ/mol. According to the chitin thermogram (Fig. 2.a), this interval belonged to degradation of GlcNAc units in the polymer. In 67% conversion, for both studied methods, there was a peak that, in agreement with TGA measurement (Fig. 2.a), is a transition between the degradation described above and the total degradation of chitosan ring and decomposition of the residual carbon ($\alpha > 70\%$, $E_a \approx 130$ kJ/mol) [9,43].

For the C54 sample, note that there were significant differences between this curve and the remaining chitosan samples, since this sample exhibited an extend peak from 5% to 65% conversion for both methods. In the FWO method, for conversions up to 27% (where the peak is localized) the activation energy increased from 120 to 152 kJ/mol. Similarly, for VYA method, until conversion of 22%, the activation energy raises from 152 to 203 kJ/mol. These conversion intervals were corresponded with the second peak of the TGA test, i.e. with the degradation of Glc units of the C54 sample. These results were similar to those found for chitin in this work and in literature (~150 kJ/mol) [45–47]. From 27 and 22% until 66 and 63% (for FWO and VYA, respectively), the activation energy decreased until a mean value of 100 kJ/mol, in both methods. In this case, the reaction stage that took place was the degradation of the GlcNAc units, corresponding with the third stage of the TGA. In the studied methods, from 66 and 63%, for FWO and VYA, respectively, to 95%, occurred the rest of the decomposition of the polymer.

The behavior of the activation energy as a function of the conversion is similar for the chitosans C62, C69, C77 and C84 (Fig. 3). First, these samples presented an increase in the activation energy up to a maximum; then, the activation energy decreased until a constant value (between 90 and 120 kJ/mol). The maximum of the activation energies for C62 and C77 samples was 192 kJ/mol (for conversions of 38 and 42%, respectively) by the FWO method. For the same method, the C69 and C84 sample showed maxima of 201 and 148 kJ/mol (at the same conversion of 40%), respectively. However, by the VYA method, the maxima for these samples were 270, 287, 319, and 207 kJ/mol with conversions of 34, 37, 40 and 33% for C62, C69, C77, and C84, respectively. According to the results of TGA analysis, the overlapped degradation reactions of Glc and GlcNAc units of these samples started at 1% and ended at 60% of conversion, so that, unlike in the case of C54, it was not possible to distinguish the activation energies corresponding to these stages with the FWO and VYA methods, which evidences the difference of the degradation mechanism of C54 and the other chitosans. From 60 until 95%, the activation energy remained constant between 62–125 kJ/mol for chitosans C62-C84 due to the same reasons that the C54 sample. It is noted that the thermal behavior of C54 sample presented an intermediate behavior between that of the chitin and the rest of obtained chitosans, being nearer to that shown by chitin than the remaining chitosans, supported by both the shape of the curves of the activation energies with conversion (Fig. 3), the TGA thermograms (Fig. 2), and the results of the thermal stabilities (Table 1).

The obtained values of the activation energies of the chitosans

Table 1
Values of $T_{25\%}$ at different heating rates and CrI for chitin raw material and obtained chitosans (mean values ± SD, n = 3).

Sample	$T_{25\%}$					CrI (%)
	6 °C/min	8 °C/min	10 °C/min	12 °C/min	14 °C/min	
Chitin	309.9 ± 0.5	314.7 ± 0.1	319.8 ± 0.3	321.8 ± 0.6	325.1 ± 0.1	95.7 ± 1.9
C54	298.5 ± 1.8	304.2 ± 0.1	308.4 ± 0.6	311.2 ± 1.7	313.7 ± 0.8	89.6 ± 2.3
C62	289.2 ± 1.0	294.7 ± 0.1	297.3 ± 0.3	300.4 ± 0.6	302.7 ± 0.4	82.6 ± 3.3
C69	286.0 ± 0.1	290.6 ± 0.2	293.9 ± 0.7	297.2 ± 0.5	298.2 ± 1.0	73.6 ± 2.9
C77	288.4 ± 1.0	291.7 ± 0.5	296.2 ± 0.2	299.4 ± 0.7	301.9 ± 0.5	72.3 ± 2.9
C84	289.1 ± 1.1	295.3 ± 0.4	299.7 ± 0.2	303.5 ± 0.3	305.7 ± 0.2	75.7 ± 3.0

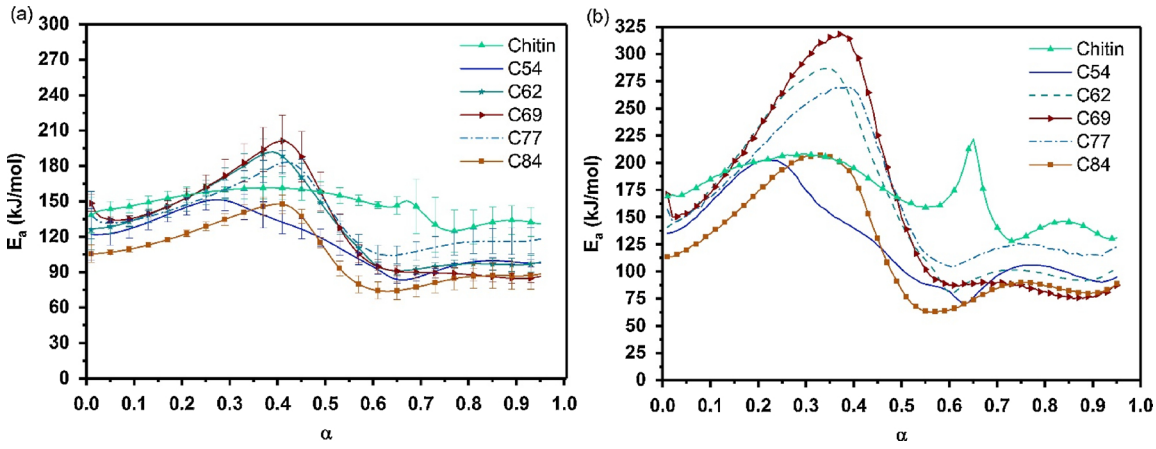

Fig. 3. Activation energy as function of conversion of all chitosans and chitin by applying the FWO (a) and VYA (b) methods.

Table 2
Activation energies obtained of chitosans by isoconversional methods in literature and this work in air atmosphere.

DD (%)	Method	Activation energy (kJ/mol)		Reference
		< 60% conversion	> 60% conversion	
≥ 75	KAS[a]	126[b]	99.1[b]	[47]
92	FWO	120.5[b]	109.6[b]	[13]
92	CR[c]	117.3 [b]	102.8 [b]	[13]
54-84	FWO	75-201	86-116	This work
54-84	VYA	62-319	80-125	This work

[a] Kissinger-Akahira-Sunose [48].
[b] Average value.
[c] Coats-Redfern method [49].

degradations of 75–201 kJ/mol and 62–319 kJ/mol for FWO and VYA, respectively, are consistent with the mean values of the isoconversional methods applied for other authors for different isoconversional methods (Table 2), being these activation energies between 117.3-126 kJ/mol for the conversions until 60%, and 99.1-109.6 kJ/mol for conversions above 60% at different DD.

4.3.2. 3R-Gaussian DAEM model

According to TGA and DTG curves, three reaction steps took place in the degradation process on dry basis. For this reason, a 3R-Gaussian DAEM model was applied to the experimental data (Eq. 9). The experimental results of the DAEM models and their derivative curves for C54 and C84 samples are showed in Fig. 4, as well as the normalized contributions of each of the reaction stages are also included.

According to the Fig. 4.a–b, the first step (degradation of the Glc units) was given from 1 to 30% of conversion for C54 sample, and of 1 to 44% of the degradation process for C84 sample. However, the second reaction stage, corresponding with the degradations of the GlcNAc units, occurred between the 6 and 64% for C54 sample, and the 7 and 60% for C84 sample. In the case of the third reaction step, this began in a conversion of 12 and 5% for C54 and C84 sample, respectively; and ended in a 97% of the degradation process for both samples.

The parameters of the 3R-Gaussian DAEM model for each sample, mean activation energy (E_{aj}) and standard deviation (σ_j) of each distribution, and contribution of each reaction stage (c_j), together with the logarithm of the pre-exponential factors and mean square error (MSE), are shown in Table 3.

The MSE values confirmed the good fit of the experimental data and the model used. In general, both the activation energies and the pre-exponential factors obtained from to the all degradation reactions did not show a clear trend with the DD of the samples (as shown in Table 3). The mean activation energies for the first and second degradation stages of chitin were the same (i.e. there was an overlapping of the first and second distributions of activation energies), indicating that the model is indeed splitting into two stages a single stage, because of the utilization of 3R-Gaussian DAEM model (deconvolution of a single stage into two stages is somehow forced because of model). In this case a 2R-Gaussian DAEM model could perfectly describe the thermal degradation of chitin. The reason of this is because the low amount of Glc units contained in chitin (only 5.2%); thus, the contribution of these units was negligible in the thermal degradation of chitin for 3R-Gaussian DAEM model.

As can be observed in Fig. 4.a–b, and specifically in Table 3, the contributions of the first (c_1) and second (c_2) reaction stages to the degradation process of the C54 and C84 were different. For the C54 sample, the first step had the least contribution (0.195), followed by the second (0.384), which had more contribution to the process than the first stage. The same tendency was found for chitin, confirming that the mechanism of degradation of this sample was similar to the degradation behavior of C54 sample. This trend did not occur in C84 sample (c_1 = 0.332; c_2 = 0.166), due to that this sample had a higher content in Glc units than the C54 (related to the first reaction step).

The cumulative distribution functions and the probability density functions for C54 and C84 samples, for each distribution function, are shown in Fig. 5.

The third distribution function (associated with the third reaction stage of degradation) exhibited wide ranges of the activation energy values (Fig. 5.b and c), followed by the second distribution function. These functions were wider than those contributed by the first distribution function, note that the standard deviations for the Gaussian curves in Table 3 were higher for the third distribution than for the others (σ values of 19.1 and 42.2 for C54 and C84, respectively), which also occurred for the C77 sample (σ = 35.1). However, for the C62 and C69 chitosans, this fact was not presented, being the standard deviations of the third functions lower than of the second ones. The low values of the standard deviations of the first reaction step for all samples suggest that this reaction occurs in a single step (Table 3 and Fig. 5.b and d).

In contrast to the isoconversional methods, with the 3R-Gaussian DAEM model was possible to acquire the activation energies related to each reaction stages of the degradation process for all chitosans, despite the overlapped of first and second reaction steps. The obtained data for the activation energies by this model for the first and second reaction steps (between 175 and 345 kJ/mol for all chitosans) were agreement, to a greater extent, with those obtained by VYA method (100–319 kJ/mol) than of with the FWO method (100–201 kJ/mol). Because of this and the VYA method is more accurate than the FWO (due to directly numerical integration), the proposed DAEM model was also more precise. On the other hand, the activation energies of the third reaction

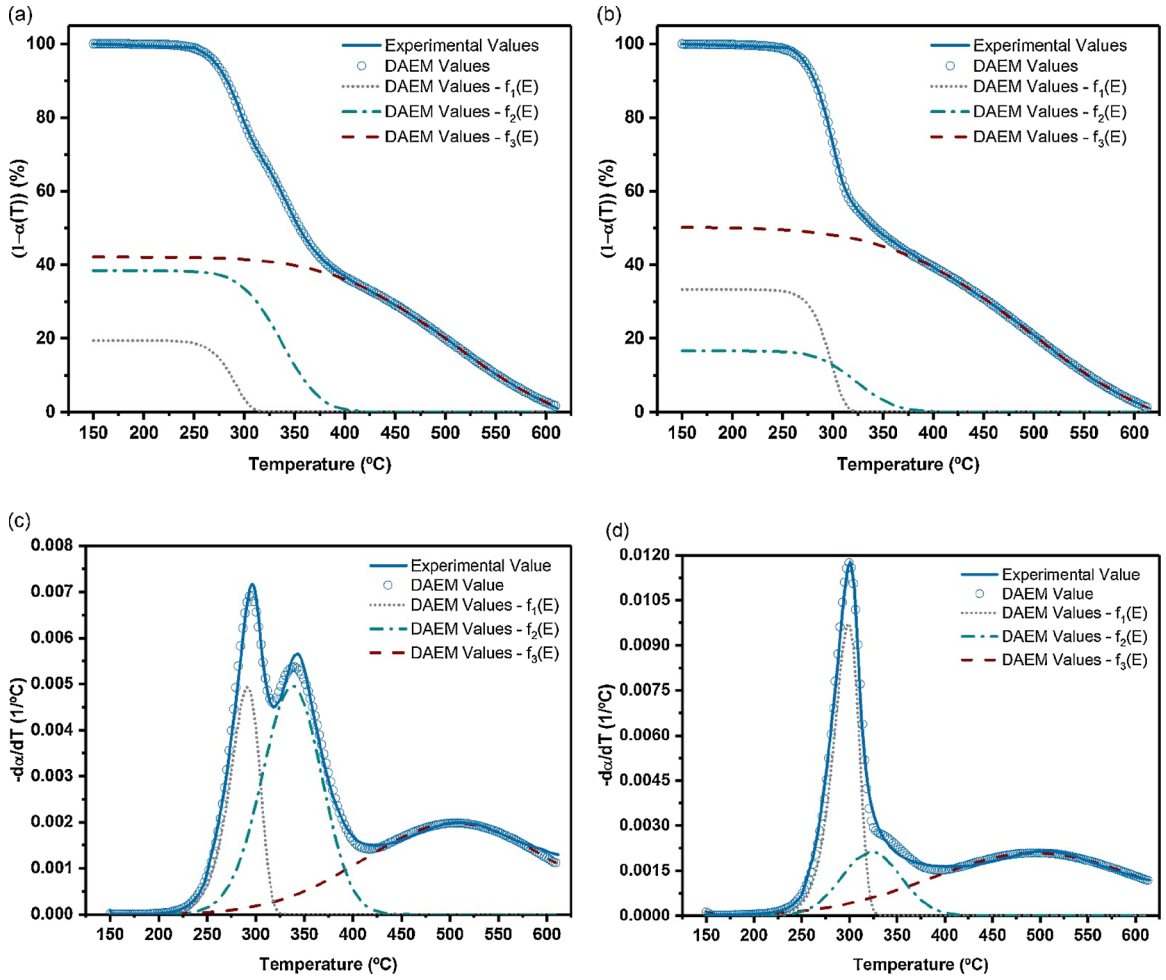

Fig. 4. Distributed activation energy model (DAEM) predictions for conversion of the C54 (a) and C84 (b) and their derivatives, (c) and (d), respectively.

Table 3
Kinetic parameters of the thermal degradation of chitin, C54, C62, C69, C77, and C84 calculated by the 3R-Gaussian DAEM model.

Parameters	Chitin	C54	C62	C69	C77	C84
Ea_1 (kJ/mol)	260.0	175.0	240.0	240.0	205.4	210.3
σ_1 (kJ/mol)	1.7	1.5	1.5	1.6	1.4	1.5
Ea_2 (kJ/mol)	260.4	185.8	205.6	207.8	346.3	345.0
σ_2 (kJ/mol)	10.2	7.6	27.8	28.6	17.7	17.2
Ea_3 (kJ/mol)	205.0	163.0	228.5	225.4	240.0	296.4
σ_3 (kJ/mol)	20.4	19.1	14.1	13.3	35.1	42.2
Ln (k_{01})	49.9	36.9	50.6	50.8	43.1	43.9
Ln (k_{02})	50.8	35.7	30.2	31.2	70.3	69.3
Ln (k_{03})	29.4	23.5	45.7	46.5	36.3	43.4
c_1	0.260	0.195	0.265	0.234	0.315	0.332
c_2	0.373	0.384	0.249	0.256	0.168	0.166
c_3	0.367	0.421	0.486	0.510	0.517	0.502
MSE (x 10^4)	32.00	8.52	6.06	13.00	5.43	7.43

stages were between 163 and 296.4 kJ/mol for the DAEM model, higher than that of the isoconversional methods (90–100 kJ/mol). However, the DAEM values are in agreement with the isoconversional methods of the literature (Table 2). In the same line, the pre-exponential factors are included within the ranges found by other authors, i.e. orders of magnitude from 10 to 24 [9,11,18].

For all these reasons, the proposed 3R-Gaussian DAEM model offers a great option to model the thermal degradation behavior and obtain the kinetic parameters of the stages of the degradation of chitosan in oxidizing atmosphere compared to isoconversional methods.

5. Conclusions

The thermal behavior of the chitosan degradation with different DD (54–84%) was studied in dynamic conditions under air atmosphere. The degradation of chitosan in these conditions was produced in four stages, but as DD increased, the overlap of the intermediate stages was observed, and therefore three stages could only be distinguished. The C54 chitosan presented the highest thermal stability in relation to the rest of samples studied.

The results of isoconversional methods showed a strong dependence with the conversion and ranged from 75 and 201 kJ/mol for FWO, and between 62 and 319 kJ/mol for VYA. However, with these methods were not possible to assign the values of the activation energies associated to the first and second degradation reaction steps due to the overlapped between them. The 3R-Gaussian DAEM model allowed to obtain the activation energies for each one of reaction stages of thermal degradation of chitosan (E_{a1}: 175–240 kJ/mol; E_{a2}: 185.8–346.3 kJ/mol; E_{a3}: 163–296.4 kJ/mol), being this model more accurate than the isoconversional methods applied. The results showed that the 3R-Gaussian DAEM model is a suitable option for the kinetic study of the chitosan thermal degradation for any degree of deacetylation.

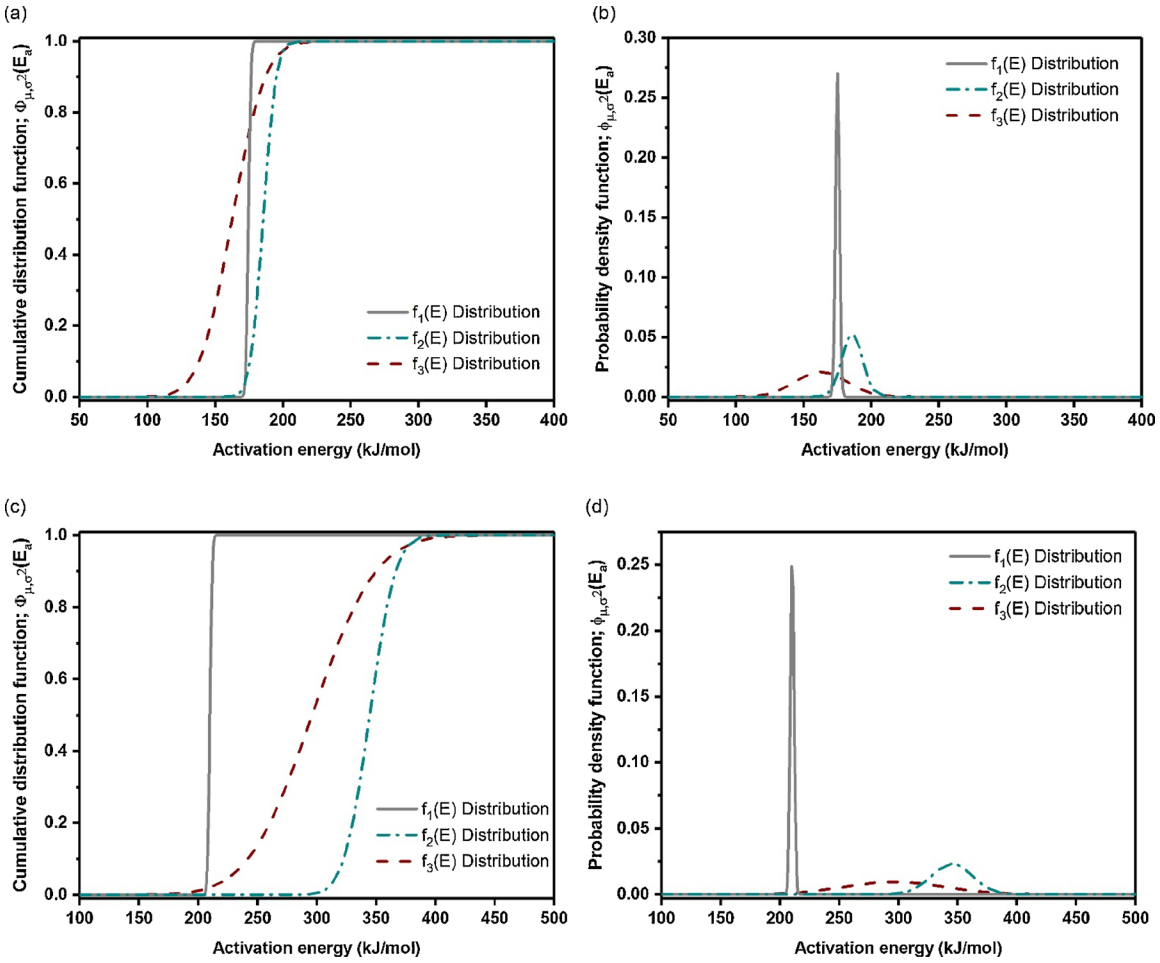

Fig. 5. Distributed activation energy model (DAEM) cumulative distribution functions of the C54 (a) and C84 (c) samples, and probability density functions: C54 (b) and C84 (d).

Acknowledgments

The authors are grateful to the "Comunidad Autónoma de Madrid" (Spain) for financial support (project S2013/MAE-2800).

Appendix A. Supplementary data

Supplementary data associated with this article can be found, in the online version, at https://doi.org/10.1016/j.tca.2018.10.004.

References

[1] I. Aranaz, M. Mengíbar, R. Harris, I. Paños, B. Miralles, N. Acosta, G. Galed, Á. Heras, Functional characterization of chitin and chitosan, Curr. Chem. Biol. 3 (2009) 203–230.
[2] A. Baranwal, A. Kumar, A. Priyadharshini, G.S. Oggu, I. Bhatnagar, A. Srivastava, P. Chandra, Chitosan: an undisputed bio-fabrication material for tissue engineering and bio-sensing applications, Int. J. Biol. Macromol. 110 (2018) 110–123.
[3] J. Wang, S. Zhuang, Removal of various pollutants from water and wastewater by modified chitosan adsorbents, Crit. Rev. Environ. Sci. Technol. 47 (2018) 2331–2386.
[4] C. Peniche, W. Argüelles-Monal, F. Goycoolea, Chitin and chitosan: major sources, properties and applications, in: M. Belgacem, A. Gandini (Eds.), Monomers, Polymers and Composites from Renewable Resources, Elsevier Ltd., 2008, pp. 517–542.
[5] K. Kurita, Controlled functionalization of the polysaccharide chitin, Prog. Polym. Sci. 26 (2001) 1921–1971.
[6] G.A.F. Roberts, Chitin Chemistry, Macmillan Press, London, 1992.
[7] M. Dash, F. Chiellini, R.M. Ottenbrite, E. Chiellini, Chitosan—A versatile semi-synthetic polymer in biomedical applications, Prog. Polym. Sci. 36 (2011) 981–1014.
[8] M. Rinaudo, Chitin and chitosan: properties and applications, Prog. Polym. Sci. 31 (2006) 603–632.
[9] H. Moussout, H. Ahlafi, M. Aazza, M. Bourakhouadar, Kinetics and mechanism of the thermal degradation of biopolymers chitin and chitosan using thermogravimetric analysis, Polym. Degrad. Stab. 130 (2016) 1–9.
[10] M.N.V.R. Kumar, A review of chitin and chitosan applications, React. Funct. Polym. 46 (2000) 1–27.
[11] D. de Britto, S.P. Campana-Filho, Kinetics of the thermal degradation of chitosan, Thermochim. Acta 465 (2007) 73–82.
[12] E. Salehi, P. Daraei, A.A. Shamsabadi, A review on chitosan-based adsorptive membranes, Carbohydr. Polym. 152 (2016) 419–432.
[13] Y.-H. Hao, Z. Huang, Q.-Q. Ye, J.-W. Wang, X.-Y. Yang, X.-Y. Fan, Y.-L. Li, Y.-W. Peng, A comparison study on non-isothermal decomposition kinetics of chitosan with different analysis methods, J. Therm. Anal. Calorim. 128 (2017) 1077–1091.
[14] T. Wanjun, W. Cunxin, C. Donghua, Kinetic studies on the pyrolysis of chitin and chitosan, Polym. Degrad. Stab. 87 (2005) 389–394.
[15] J. Zawadzki, H. Kaczmarek, Thermal treatment of chitosan in various conditions, Carbohydr. Polym. 80 (2010) 394–400.
[16] F. López, A. Mercê, F. Alguacil, A. López-Delgado, A kinetic study on the thermal behaviour of chitosan, J. Therm. Anal. Calorim. 91 (2008) 633–639.
[17] L. Zeng, C. Qin, L. Wang, W. Li, Volatile compounds formed from the pyrolysis of chitosan, Carbohydr. Polym. 83 (2011) 1553–1557.
[18] M. Gámiz-González, D.M. Correia, S. Lanceros-Mendez, V. Sencadas, J.G. Ribelles, A. Vidaurre, Kinetic study of thermal degradation of chitosan as a function of deacetylation degree, Carbohydr. Polym. 167 (2017) 52–58.
[19] Y. Qiao, S. Chen, Y. Liu, H. Sun, S. Jia, J. Shi, C.M. Pedersen, Y. Wang, X. Hou, Pyrolysis of chitin biomass: TG–MS analysis and solid char residue characterization, Carbohydr. Polym. 133 (2015) 163–170.
[20] Y.S. Nam, W.H. Park, D. Ihm, S.M. Hudson, Effect of the degree of deacetylation on the thermal decomposition of chitin and chitosan nanofibers, Carbohydr. Polym. 80 (2010) 291–295.
[21] S. Vyazovkin, A.K. Burnham, J.M. Criado, L.A. Pérez-Maqueda, C. Popescu, N. Sbirrazzuoli, ICTAC Kinetics Committee recommendations for performing kinetic computations on thermal analysis data, Thermochim. Acta 520 (2011) 1–19.
[22] T. Ozawa, A new method of analyzing thermogravimetric data, Bull. Chem. Soc. Jpn. 38 (1965) 1881–1886.
[23] J.H. Flynn, L.A. Wall, General treatment of the thermogravimetry of polymers, J.

Res. Nat. Bur. Stand. 70A (1966) 487–523.
[24] S. Vyazovkin, Evaluation of activation energy of thermally stimulated solid-state reactions under arbitrary variation of temperature, J. Comput. Chem. 18 (1997) 393–402.
[25] S. Vyazovkin, Modification of the integral isoconversional method to account for variation in the activation energy, J. Comput. Chem. 22 (2001) 178–183.
[26] S. Vyazovkin, D. Dollimore, Linear and nonlinear procedures in isoconversional computations of the activation energy of nonisothermal reactions in solids, J. Chem. Inf. Comput. Sci. 36 (1996) 42–45.
[27] K. Muraleedharan, P. Alikutty, V.A. Mujeeb, K. Sarada, Kinetic studies on the thermal dehydration and degradation of chitosan and citralidene chitosan, J. Polym. Environ. 23 (2015) 1–10.
[28] V. Vand, A theory of the irreversible electrical resistance changes of metallic films evaporated in vacuum, Proc. Phys. Soc. 55 (1943) 222.
[29] G. Pitt, The kinetics of the evolution of volatile products from coal, Fuel 41 (1962) 267–274.
[30] J. Cai, T. Li, R. Liu, A critical study of the Miura–Maki integral method for the estimation of the kinetic parameters of the distributed activation energy model, Bioresour. Technol. 102 (2011) 3894–3899.
[31] W. Wu, Y. Mei, L. Zhang, R. Liu, J. Cai, Effective activation energies of lignocellulosic biomass pyrolysis, Energy Fuels 28 (2014) 3916–3923.
[32] J. Cai, W. Wu, R. Liu, G.W. Huber, A distributed activation energy model for the pyrolysis of lignocellulosic biomass, Green Chem. 15 (2013) 1331–1340.
[33] M.H. Ottey, K.M. Vårum, O. Smidsrød, Compositional heterogeneity of heterogeneously deacetylated chitosans, Carbohydr. Polym. 29 (1996) 17–24.
[34] L. Raymond, F.G. Morin, R.H. Marchessault, Degree of deacetylation of chitosan using conductometric titration and solid-state NMR, Carbohydr. Res. 246 (1993) 331–336.
[35] J. Brugnerotto, J. Lizardi, F.M. Goycoolea, W. Argüelles-Monal, J. Desbrieres, M. Rinaudo, An infrared investigation in relation with chitin and chitosan characterization, Polymer 42 (2001) 3569–3580.
[36] B. Focher, P.L. Beltranme, A. Naggi, G. Torri, Alkaline *N*-deacetylation of chitin enhanced by flash treatments. Reaction kinetics and structure modifications, Carbohydr. Polym. 12 (1990) 405–418.
[37] J. Cai, R. Liu, Weibull mixture model for modeling nonisothermal kinetics of thermally stimulated solid-state reactions: application to simulated and real kinetic conversion data, J. Phys. Chem. B 111 (2007) 10681–10686.
[38] M. Duarte, M. Ferreira, M. Marvao, J. Rocha, An optimised method to determine the degree of acetylation of chitin and chitosan by FTIR spectroscopy, Int. J. Biol. Macromol. 31 (2002) 1–8.
[39] J. Singh, P. Dutta, J. Dutta, A. Hunt, D. Macquarrie, J. Clark, Preparation and properties of highly soluble chitosan–l-glutamic acid aerogel derivative, Carbohydr. Polym. 76 (2009) 188–195.
[40] A. Pawlak, M. Mucha, Thermogravimetric and FTIR studies of chitosan blends, Thermochim. Acta 396 (2003) 153–166.
[41] V. Gomez-Serrano, J. Pastor-Villegas, A. Perez-Florindo, C. Duran-Valle, C. Valenzuela-Calahorro, FT-IR study of rockrose and of char and activated carbon, J. Anal. Appl. Pyrolysis 36 (1996) 71–80.
[42] I. Corazzari, R. Nisticò, F. Turci, M.G. Faga, F. Franzoso, S. Tabasso, G. Magnacca, Advanced physico-chemical characterization of chitosan by means of TGA coupled on-line with FTIR and GCMS: thermal degradation and water adsorption capacity, Polym. Degrad. Stab. 112 (2015) 1–9.
[43] A. Martínez-Camacho, M. Cortez-Rocha, J. Ezquerra-Brauer, A. Graciano-Verdugo, F. Rodriguez-Félix, M. Castillo-Ortega, M. Yépiz-Gómez, M. Plascencia-Jatomea, Chitosan composite films: thermal, structural, mechanical and antifungal properties, Carbohydr. Polym. 82 (2010) 305–315.
[44] E.S. Abdou, K.S. Nagy, M.Z. Elsabee, Extraction and characterization of chitin and chitosan from local sources, Bioresour. Technol. 99 (2008) 1359–1367.
[45] V. Georgieva, D. Zvezdova, L. Vlaev, Non-isothermal kinetics of thermal degradation of chitin, J. Therm. Anal. Calorim. 111 (2013) 763–771.
[46] P. Stolarek, S. Ledakowicz, Pyrolysis kinetics of chitin by non-isothermal thermogravimetry, Thermochim. Acta 433 (2005) 200–208.
[47] V. Georgieva, D. Zvezdova, L. Vlaev, Non-isothermal kinetics of thermal degradation of chitosan, Chem. Cent. J. 6 (2012) 81.
[48] T. Akahira, T. Sunose, Method of determining activation deterioration constant of electrical insulating materials, Res. Rep. Chiba Inst. Technol. 16 (1971) 22–31.
[49] A.W. Coats, J. Redfern, Kinetic parameters from thermogravimetric data, Nature 201 (1964) 68.